X-ray Magnetic Circular and Linear Dichroism (XMCD, XMLD)

and

X-ray Magnetic Imaging (PEEM, ...)

Jan Vogel
Institut Néel (CNRS, UJF), Nanoscience Department
Grenoble, France

- X-ray (Magnetic) Circular and Linear Dichroism in Absorption
- Sum rules: determination of orbital and spin moments
- XMCD and XMLD for element-selective magnetic imaging

X-ray Absorption Spectroscopy

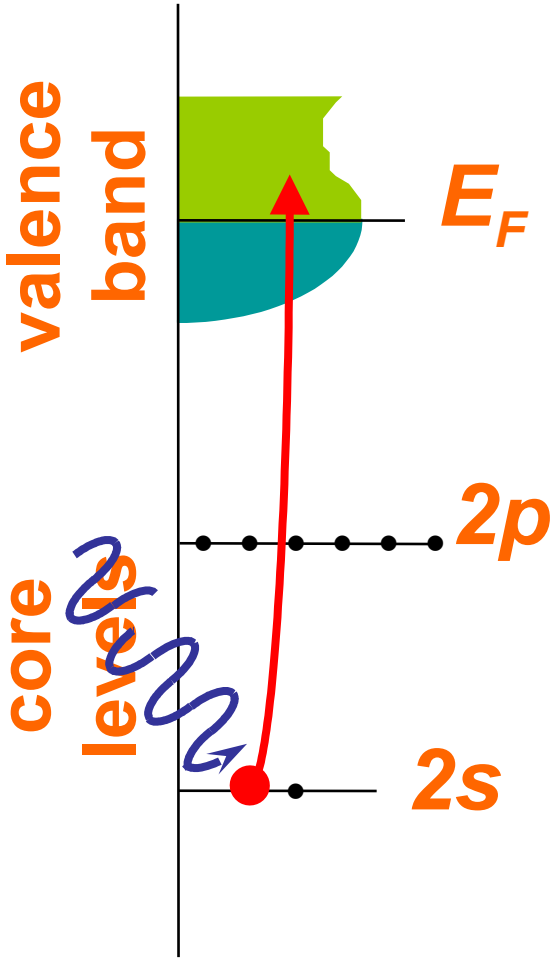

X-ray Absorption Spectroscopy

K-edge: 1s → empty *p*-states

L_1-edge: 2s → empty *p*-states

$L_{2,3}$-edges: $2p_{1/2,\ 3/2}$ → empty *d*-states

$M_{4,5}$-edges: $3d_{3/2,\ 5/2}$ → empty *f* -states

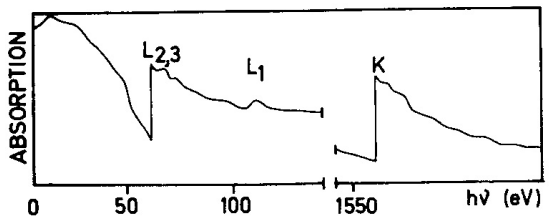

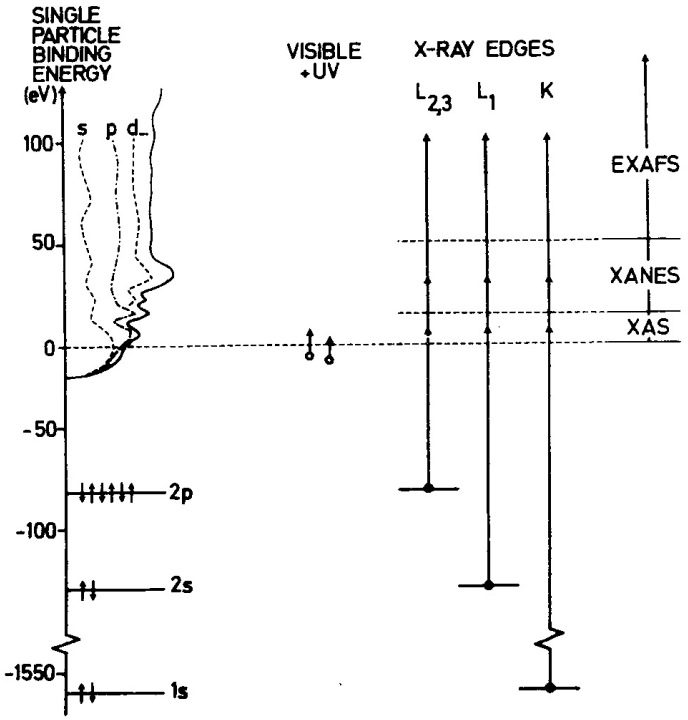

Spin-orbit coupling: $l \geq 1$

Spin parallel/anti-parallel to orbit:

$j = l + s,\ l - s$

$p \rightarrow 1/2,\ 3/2$ $\qquad$ $d \rightarrow 3/2,\ 5/2$

Branching ratios: $-j \leq m_j \leq j$

$p_{1/2} \rightarrow m_j = -1/2,\ 1/2$

$p_{3/2} \rightarrow m_j = -3/2,\ -1/2,\ 1/2,\ 3/2$

Intensity ratio $p_{3/2} : p_{1/2} = 2 : 1$

$d_{5/2} : d_{3/2} = 3 : 2$

NÉEL institut

cnrs

Detection of X-ray Absorption Spectroscopy

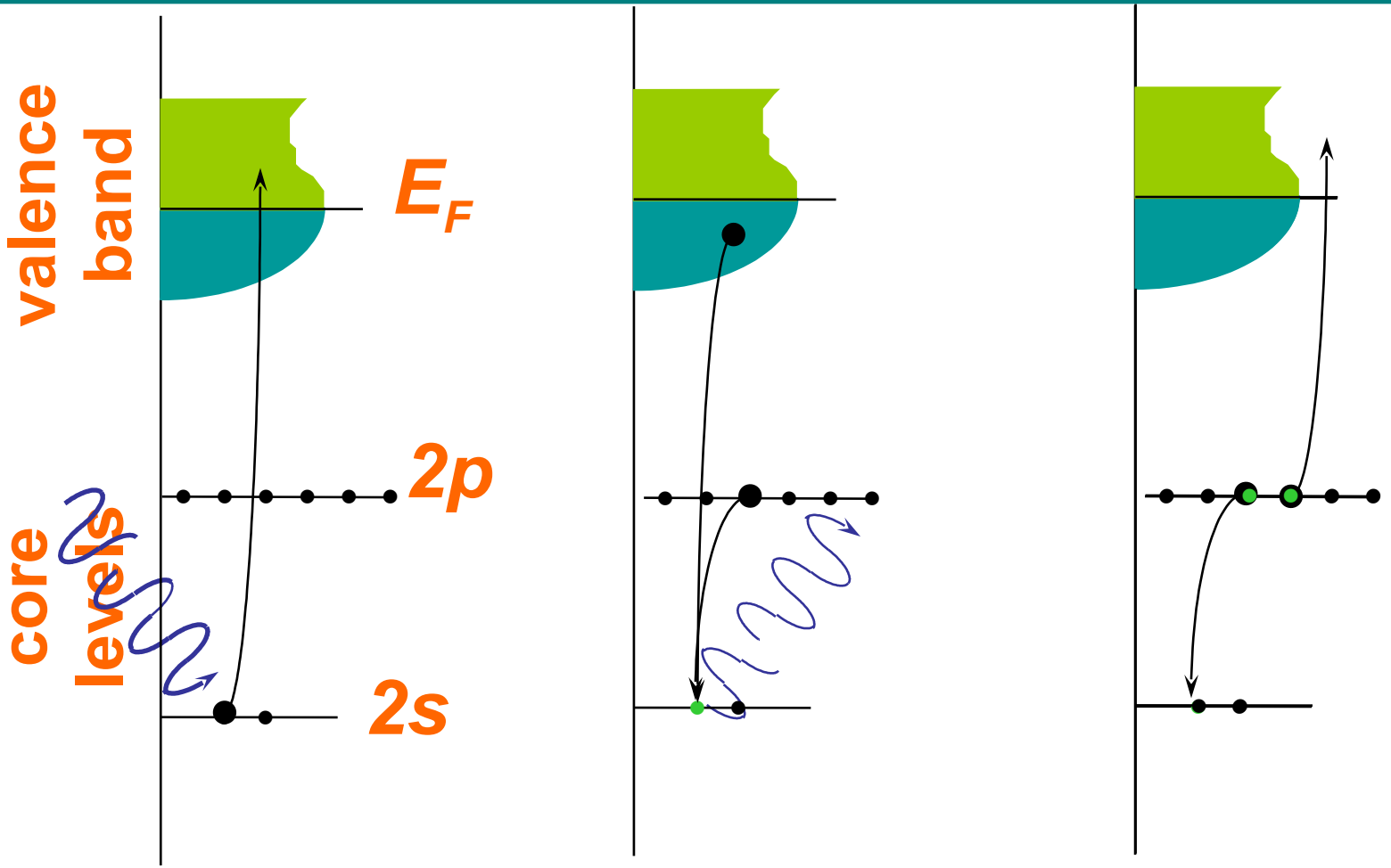

Typical timescales 10^{-15} s

Fluorescence
(radiative decay)

Auger decay
(non-radiative decay)

X-ray Dichroism in Absorption

Polarization dependence of X-ray Absorption Spectra

X-ray Magnetic Circular Dichroism (XMCD): difference in absorption for left- and right circularly polarized light.

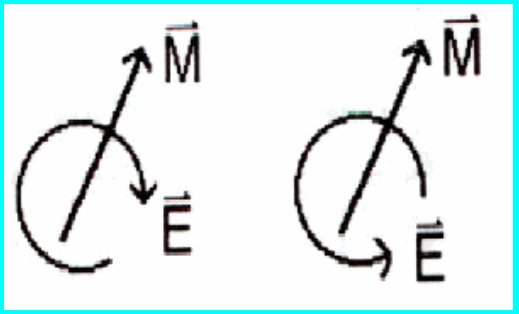

X-ray Linear Dichroism: difference in absorption for linearly polarized light ⊥ and // to quantization axis.

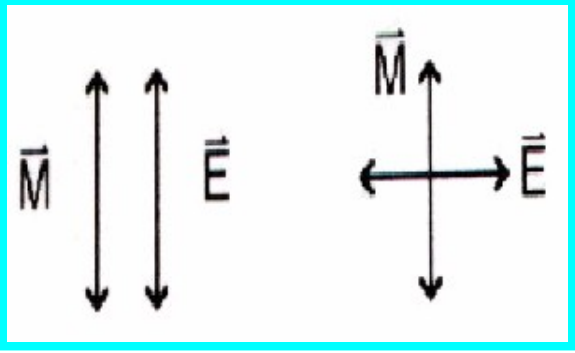

X-ray Dichroism in Absorption : history

1846 - **M. Faraday**: polarisation of visible light changes when transmitted by a magnetic material

1975 - **Erskine and Stern** - first theoretical formulation of XMCD effect
excitation from a core state to a valence state for the $M_{2,3}$ edge of Ni.

1985 - Thole, van de Laan, Sawatzky - first calculations of XMLD for rare earth materials

1986- van der Laan - first experiment of XMLD

1987 - G. Schütz et al. - first experimental demonstration of the XMCD at the K-edge of Fe

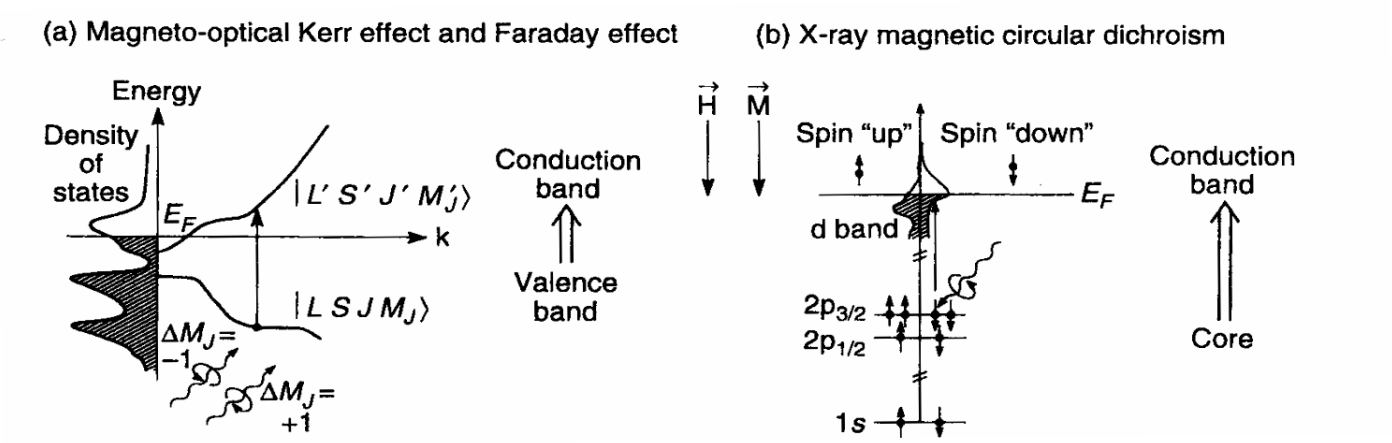

X-ray Absorption Edges and Magnetism

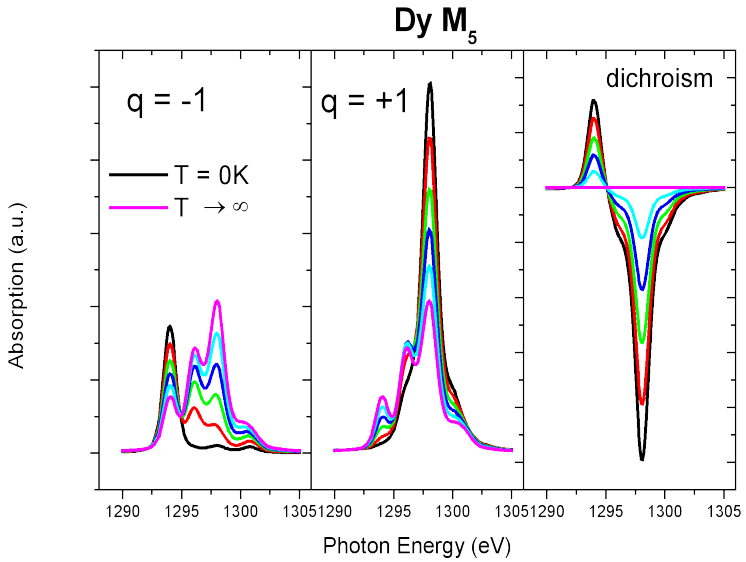

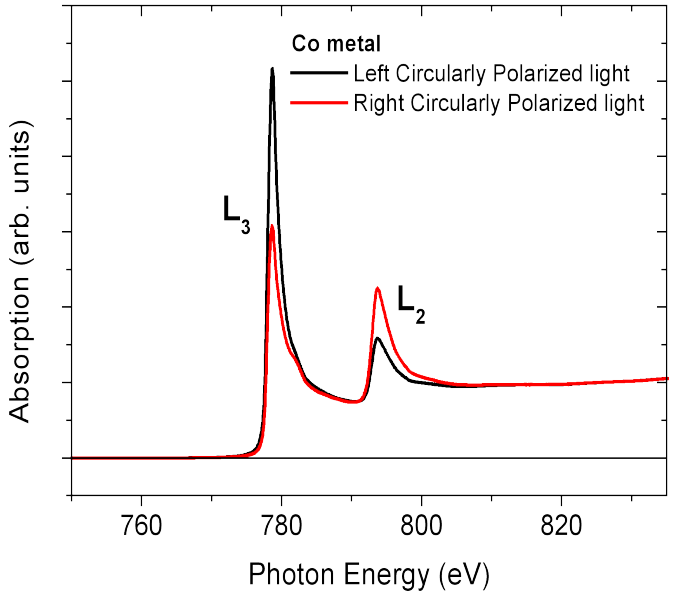

Rare Earths (4f materials) :

$M_{4,5}$-edges ($3d \rightarrow 4f$)

$L_{2,3}$-edges ($2p \rightarrow 5d$)

Transition Metals

$L_{2,3}$-edges ($2p \rightarrow 3d$)

K-edge ($1s \rightarrow 4p$)

X-ray Absorption Spectroscopy

Absorption cross-section :

$w_{abs} = (2\pi/h) \; |< \Phi_f |T| \Phi_i >|^2 \; \rho_f(E_{h\nu} - E_i)$ Fermi 's Golden Rule

One electron approximation : multiple scattering and band-structure effects dominate the spectra
Transitions to delocalized states ($L_{2,3}$ of metallic 3d, K-edges)

Many-body approximation (multiplets) : spectra dominated by e^- - e^- and electron-hole interactions.
Transitions to localized states ($L_{2,3}$ of ionic 3d, Rare-Earth $M_{4,5}$)

X-ray Absorption Spectroscopy : many-body effects

Atomic wavefunctions: $\langle \Phi_f | \mathbf{e}_q \cdot \mathbf{r} | \Phi_i \rangle \Rightarrow \langle \phi\,(J'M') | \mathbf{e}_q \cdot \mathbf{r} | \phi\,(JM) \rangle$

(q = polarization of light)

Wigner-Eckhart theorem:

$$\langle \phi\,(J'M') | P_q | \phi\,(JM) \rangle = (-1)^{J-M} \begin{pmatrix} J & 1 & J' \\ -M & q & M' \end{pmatrix} \langle \phi\,(J') || P_q || \phi(J) \rangle$$

Selection rules :

3J symbol $\neq 0$ if: $\Delta J = (J' - J) = -1, 0, +1$ and $J' + J \geq 1$

$\Delta M = (M' - M) = q$

X-ray Absorption Spectroscopy : many-body effects

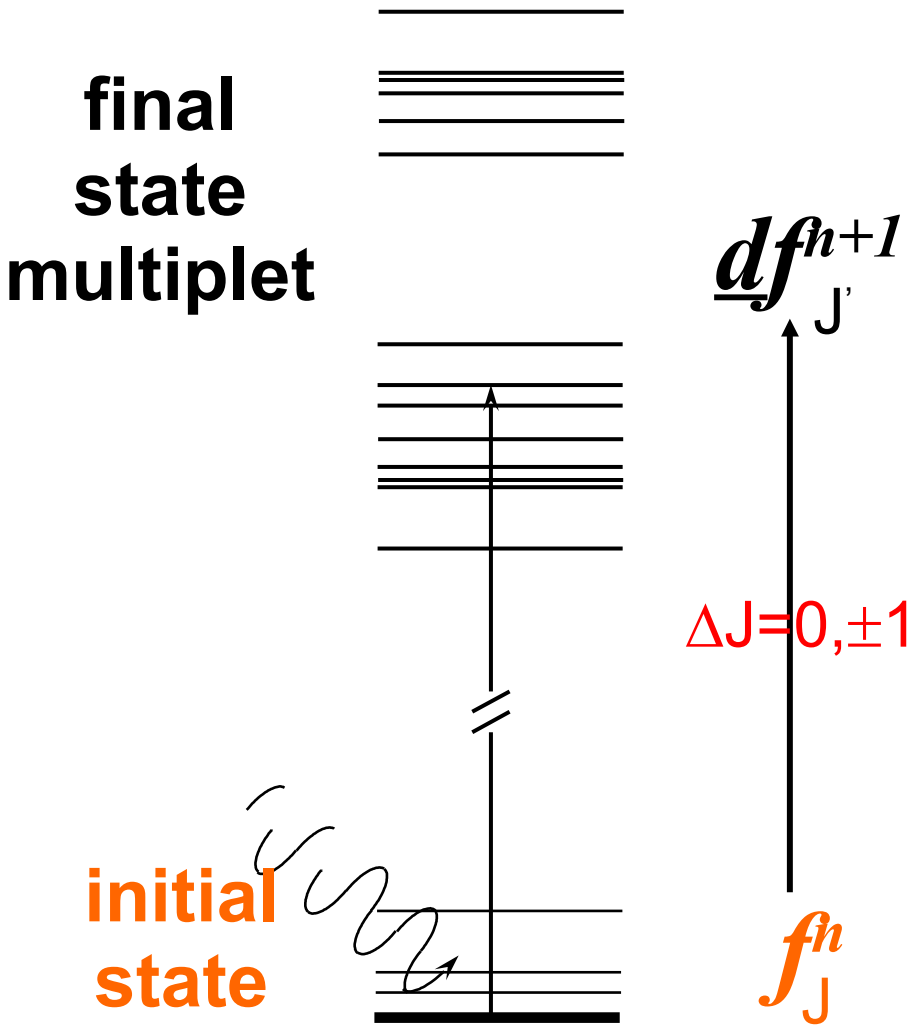

Dichroism

$\Delta J \setminus q$	-1	0	1
-1	$\frac{J(J-1)-(2J-1)M+M^2}{2J(2J+1)(2J-1)}$	$\frac{J^2-M^2}{J(2J+1)(2J-1)}$	$\frac{J(J-1)+(2J-1)M+M^2}{2J(2J+1)(2J-1)}$
0	$\frac{J(J+1)-M-M^2}{2J(2J+1)(J+1)}$	$\frac{M^2}{J(2J+1)(J+1)}$	$\frac{J(J+1)+M-M^2}{2J(2J+1)(J+1)}$
1	$\frac{(J+1)(J+2)+(2J+3)M+M^2}{2(2J+3)(2J+1)(J+1)}$	$\frac{(J+1)^2-M^2}{(2J+3)(2J+1)(J+1)}$	$\frac{(J+1)(J+2)-(2J+3)M+M^2}{2(2J+3)(2J+1)(J+1)}$

$$\begin{pmatrix} J & 1 & J' \\ -M & q & M' \end{pmatrix}^2$$

Squared 3J-symbols:

For a ground state |J,M> and for every ΔJ :

$\sigma^{q=1} - \sigma^{q=-1} \propto M$

If several M_j states are occupied: XMCD $\propto \langle M_J \rangle$

XMLD $\propto \langle M_J^2 \rangle$

- XMCD proportional to the magnetic moment of the absorbing atom
- Element selective probe of magnetic ordering

NÉEL institut

cnrs

Dichroism

Magnetic field → (2J + 1)-fold degeneracy lifted (Zeeman-splitting)

Yb ($4f^{13}$)	Hund's rules :	L = 3	S = ½	→ J = 7/2

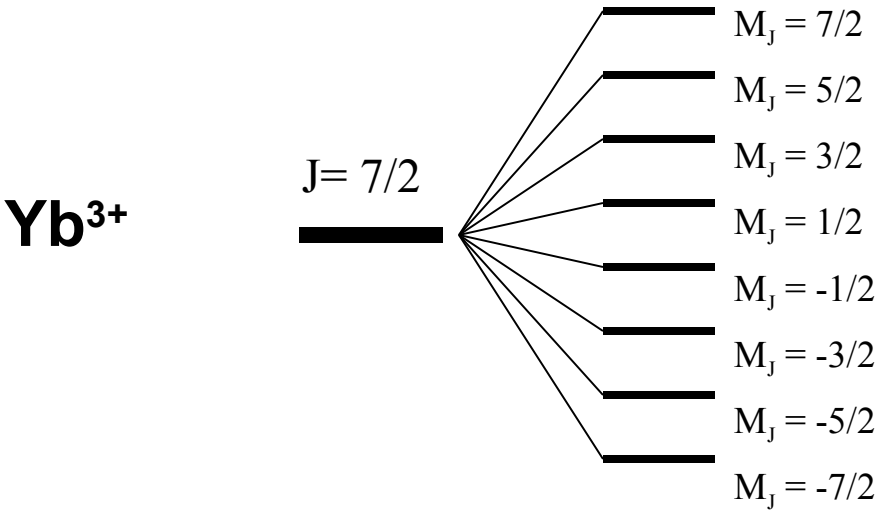

Energy of M_J - levels: $E_M = -g_{\alpha J}\mu_B H M$

Occupation of M_j-levels: **Boltzmann-distribution**

T = 0K: only lowest lying level (M_J = -J) occupied

Dichroism : Yb $M_{4,5}$- edges

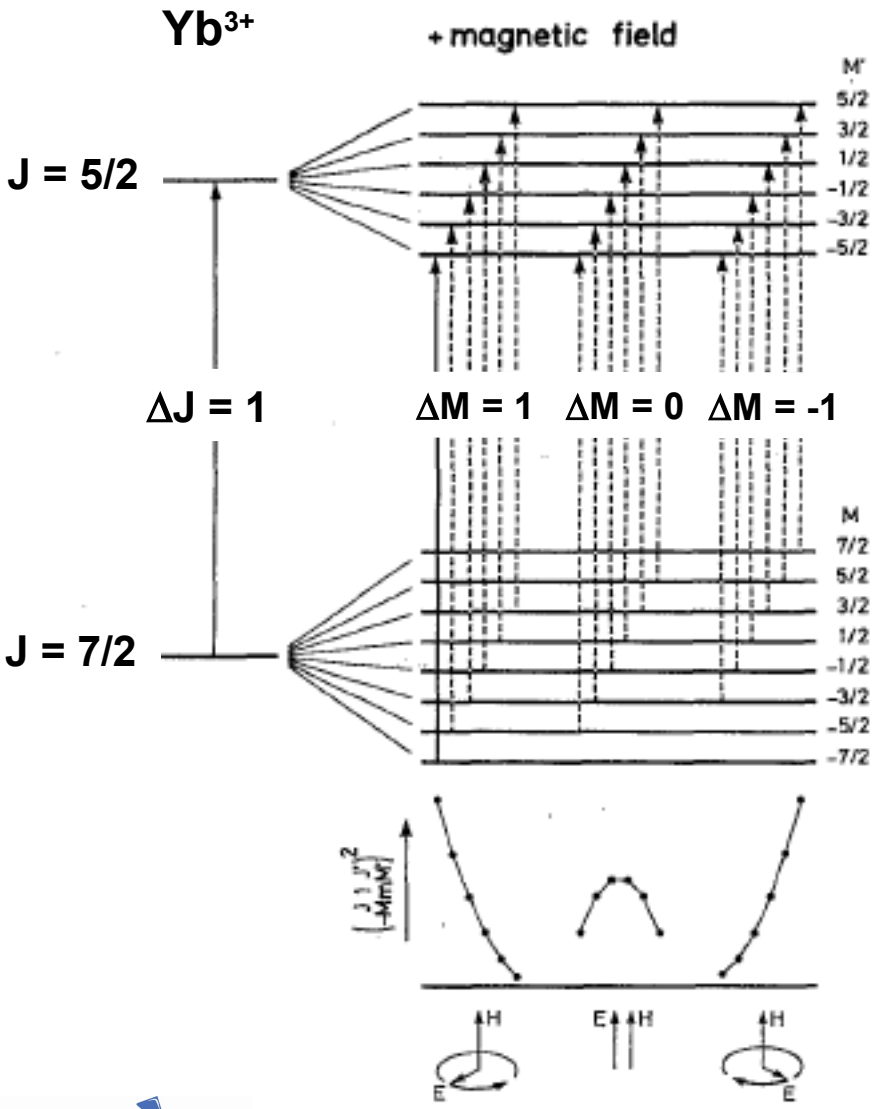

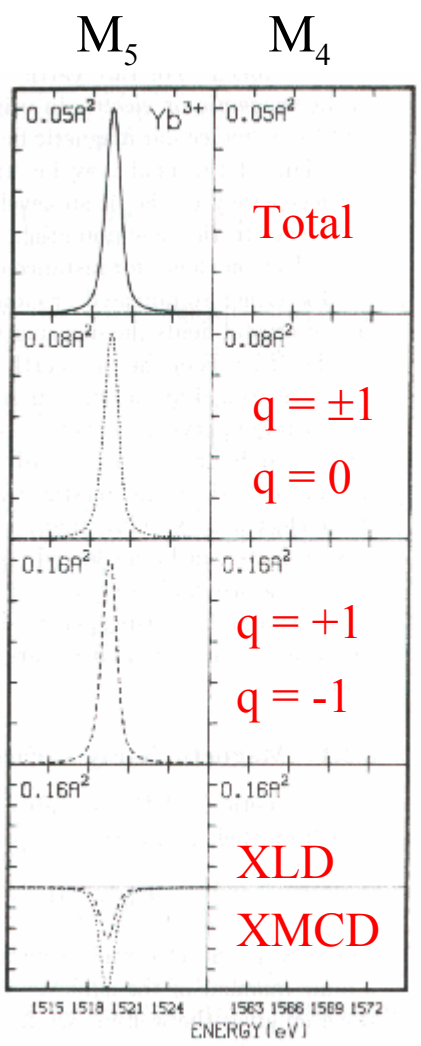

J.B. Goedkoop, Ph.D. Thesis, 1988

Dichroism : Dy $M_{4,5}$- edges

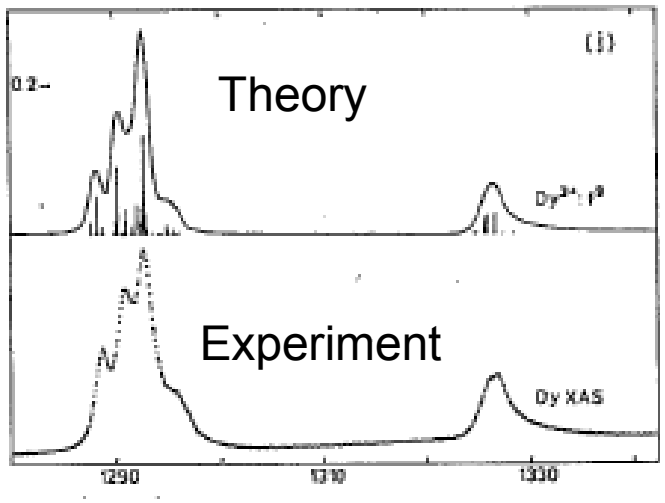

Spectra with unpolarized light

J.B. Goedkoop *et al.*, Phys. Rev. B 37, 2086 (1988).

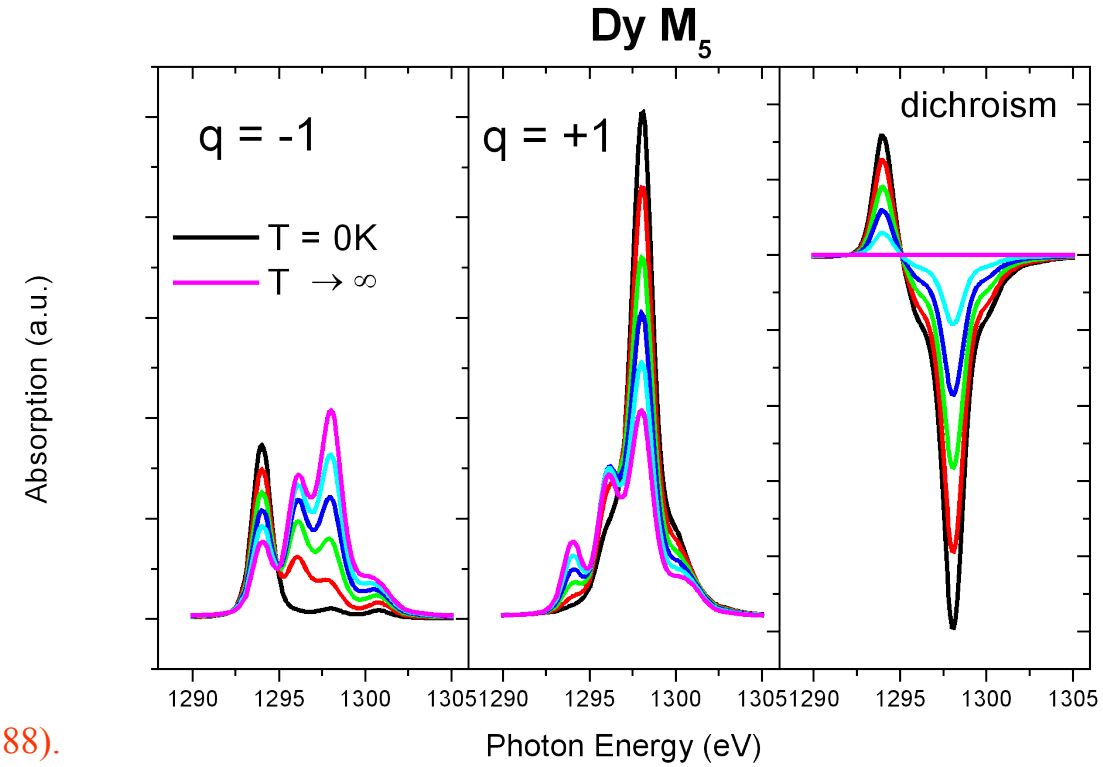

XAS spectra and XMCD vs reduced temperature
$T_R = kT / g_{\alpha J} \mu_B H$

Dichroism : delocalized states, two-step model

One electron picture: transitions from 2*p* to 3*d* band split by exchange in $3d^{\uparrow}$ and $3d^{\downarrow}$

$$|l, m_l, s, m_s\rangle = a_{ml}\, Y_{l,ml}\, |s, m_s\rangle$$

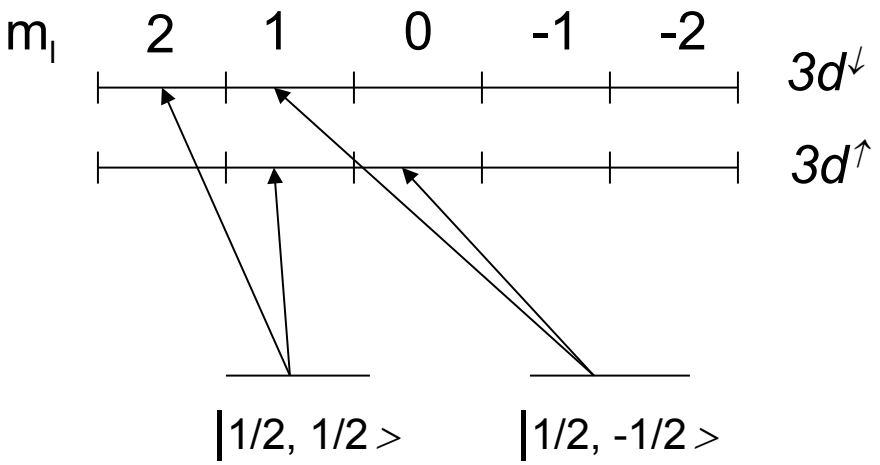

$|l,s,J,m_j\rangle$

$$\left|\tfrac{1}{2},\tfrac{1}{2}\right\rangle$$

$$\left|\tfrac{1}{2},-\tfrac{1}{2}\right\rangle$$

$|l,m_l,s,m_s\rangle$ basis

$$-\frac{1}{\sqrt{3}}Y^{\uparrow}_{10}+\frac{\sqrt{2}}{\sqrt{3}}Y^{\downarrow}_{11}$$

$$-\frac{\sqrt{2}}{\sqrt{3}}Y^{\uparrow}_{1\text{-}1}+\frac{1}{\sqrt{3}}Y^{\downarrow}_{10}$$

L_2 edge - left polarisation ($\Delta m_l = +1$)

$$I^{\uparrow} = \sum_{i,f} |\langle f|P_1|i\rangle|^2 = (1/3\ |\langle 2,1|P_1|1,0\rangle|^2 + 2/3\ |\langle 2,0|P_1|1,-1\rangle|^2)\ R^2$$

$$I^{\downarrow} = \sum |\langle f|P_1|i\rangle|^2 = (2/3\ |\langle 2,2|P_1|1,1\rangle|^2 + 1/3\ |\langle 2,1|P_1|1,0\rangle|^2)\ R^2$$

$$R = \int R_{nl}^{*}(r) R_{n'l'}(r)\, r^3 dr$$

Dichroism : delocalized states, two-step model

It can be calculated (Bethe and Salpeter) that:

$$|\langle 2,2 |P_1| 1,1\rangle|^2 = 2/5$$
$$|\langle 2,1 |P_1| 1,0\rangle|^2 = 1/5$$
$$|\langle 2,0 |P_1| 1,-1\rangle|^2 = 1/15$$

$I^{\uparrow} = 1/3(|\langle 2,1 |\mathbf{P}_1| 1,0\rangle|^2 + 2/3 |\langle 2,0 |\mathbf{P}_1| 1,-1\rangle|^2) R^2 =$
$= (1/3 * 1/5 + 2/3 * 1/15) R^2 = 1/9\ R^2$

$I^{\downarrow} = 2/3 |\langle 2,2 |\mathbf{P}_1| 1,1\rangle|^2 + 1/3 |\langle 2,1 |\mathbf{P}_1| 1,0\rangle|^2 \ R^2$
$= (2/3 * 2/5 + 1/3 * 1/5) R^2 = 1/3\ R^2$

$I^{\uparrow} / (I^{\uparrow} + I^{\downarrow}) = 0.25$ LCP at the L_2 edge
$I^{\downarrow} / (I^{\uparrow} + I^{\downarrow}) = 0.75$

$I^{\uparrow} / (I^{\uparrow} + I^{\downarrow}) = 0.75$ RCP at the L_2 edge
$I^{\downarrow} / (I^{\uparrow} + I^{\downarrow}) = 0.25$

Dichroism : delocalized states, two-step model

Step 1 : spin-polarised electrons emitted by the spin-orbit split 2p band

75% spin down and 25% spin up electrons at the L_2-edge with LCP light

37.5% spin down and 62.5% spin up electrons at the L_3-edge with LCP light

Step 2: the exchange split *d*-band acts as spin-detector.

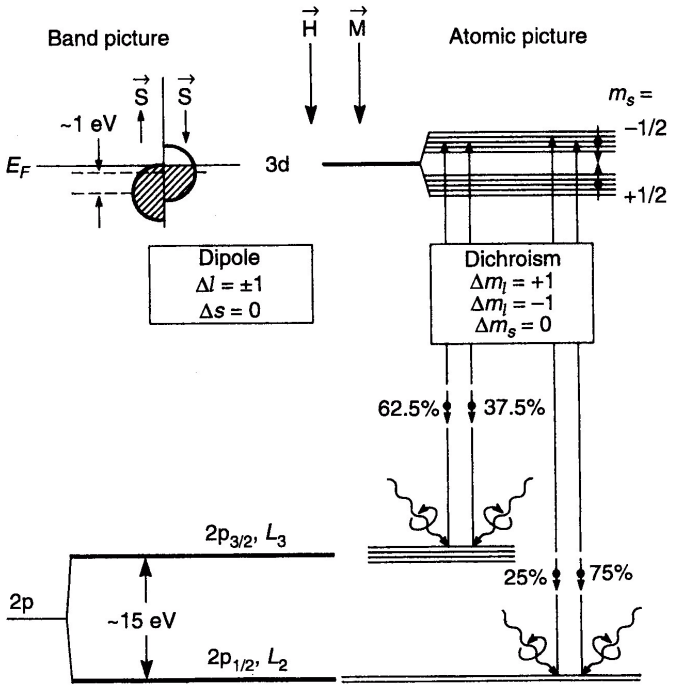

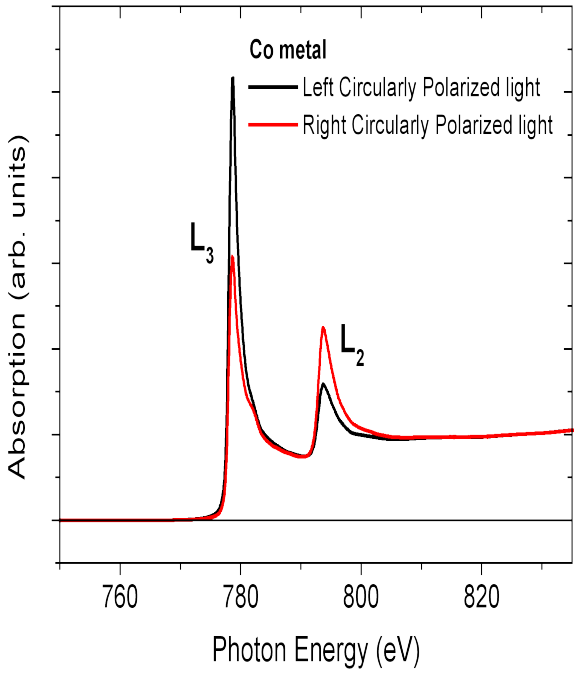

XMCD sum rules : orbital moment sum rule

Sum rules relate dichroism and total absorption to the ground-state orbital and spin magnetic moment of the probed element and shell:

$L_{2,3}$-edges of Fe $\rightarrow$ Fe 3*d*-moments.

Orbital moment sum rule:

$$\langle L_Z \rangle = [2l(l+1)(4l+2-n)]/[l(l+1)+2 - c(c+1)] \bullet$$

$$[\int_{j+ + j-} d\omega\,(\mu^+ - \mu^-) / \int_{j+ + j-} d\omega\,(\mu^+ + \mu^- + \mu^0)]$$

l = orbital quantum number of the valence state
c = orbital quantum number of the core state
n = number of electrons in the valence state

μ^+ (μ^-) = absorption spectrum for left (right) circularly polarized light.

μ^0 = absorption spectrum for linearly polarized light, with polarization parallel to quantization axis.

j^+ (j^-) = (l + 1/2) resp. (l - 1/2) absorption (ex. $2p_{3/2}$, $2p_{1/2}$)

B.T.Thole *et al.*, Phys.Rev.Lett. 68, 1943 (1992)
M.Altarelli, Phys.Rev.B 47, 597 (1993)

XMCD sum rules : orbital sum rule

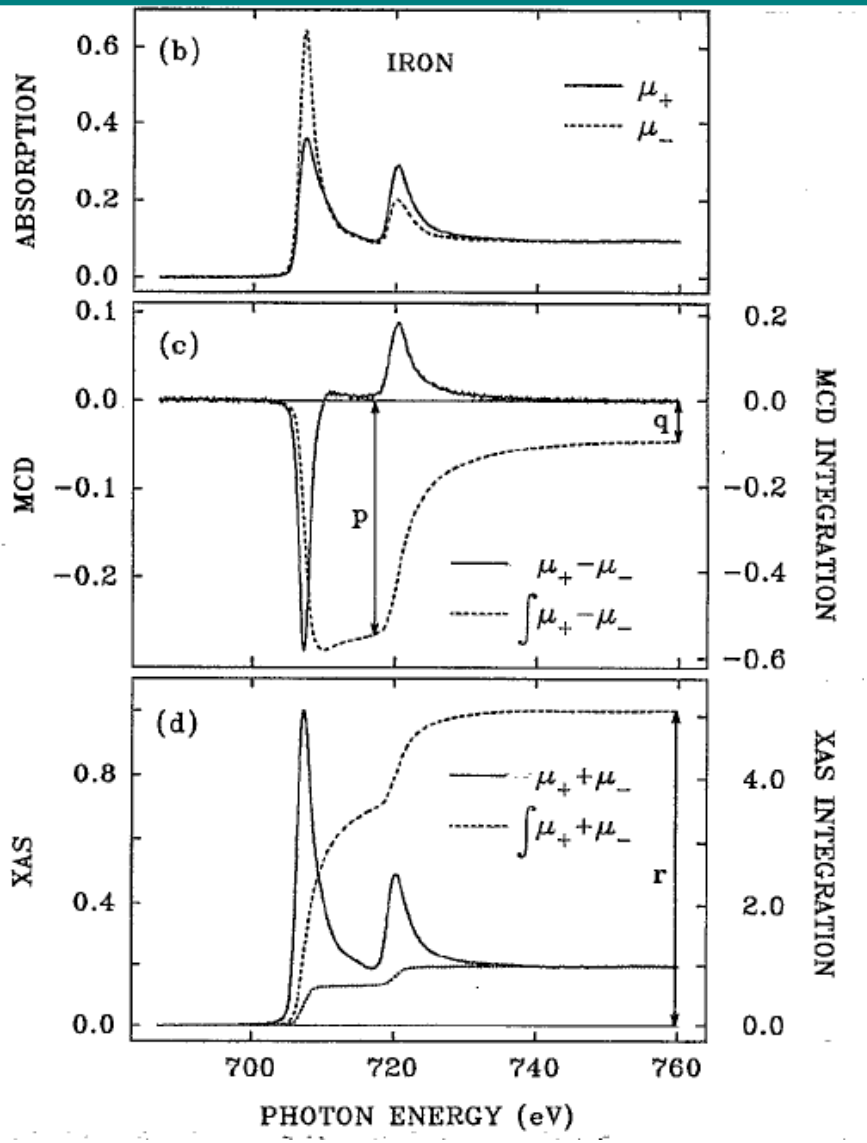

For $L_{2,3}$-edges $c = 1$ ($2p$), $l = 2$ (d):

$\langle L_Z \rangle = 2(10-n) \bullet (\Delta L_3 + \Delta L_2)$

$/ \int_{L3+L2} d\omega \, (\mu^+ + \mu^- + \mu^0)]$

$q = \Delta L_3 + \Delta L_2$

$r = \mu^+ + \mu^- = (2/3)(\mu^+ + \mu^- + \mu^0)$

$\langle L_Z \rangle = 4q\,(10-n) / 3r$

C.T.Chen *et al.*, PRL 75, 152 (1995)

XMCD sum rules : sum rule for spin moment

Spin moment sum rule

$$\langle S_Z \rangle + c_2(n) \langle T_z \rangle = c_1(n)[\int_{j+} d\omega\,(\mu^+ - \mu^-) - [(c+1)/c] \int_{j-} d\omega\,(\mu^+ - \mu^-)] / \int_{j+ + j-} d\omega\,(\mu^+ + \mu^- + \mu^0)]$$

$c_1(n) = 3c(4l + 2 - n)/[l(l+1) - 2 - c(c+1)]$

$c_2(n) = \{l(l+1)[l(l+1)+2c(c+1)+4]-3(c-1)^2(c+2)^2\} / 6lc(l+1)(4l+2-n)$

$\langle T_Z \rangle$ = expectation value of magnetic dipole operator

$T = \mathbf{S} - \mathbf{r}\,(\mathbf{r} \bullet \mathbf{s}) / r^2$

which expresses the anisotropy of the spin moment within the atom

For $L_{2,3}$-edges:

$$\langle S_Z \rangle + (7/2) \langle T_Z \rangle = (3/2)(10-n)[(\Delta L_3 - 2\Delta L_2)/ \int_{L3+L2} d\omega\,(\mu^+ + \mu^- + \mu^0)]$$

P. Carra et al., Phys. Rev. Lett. **70**, 694 (1993)

XMCD sum rules : sum rule for spin moment

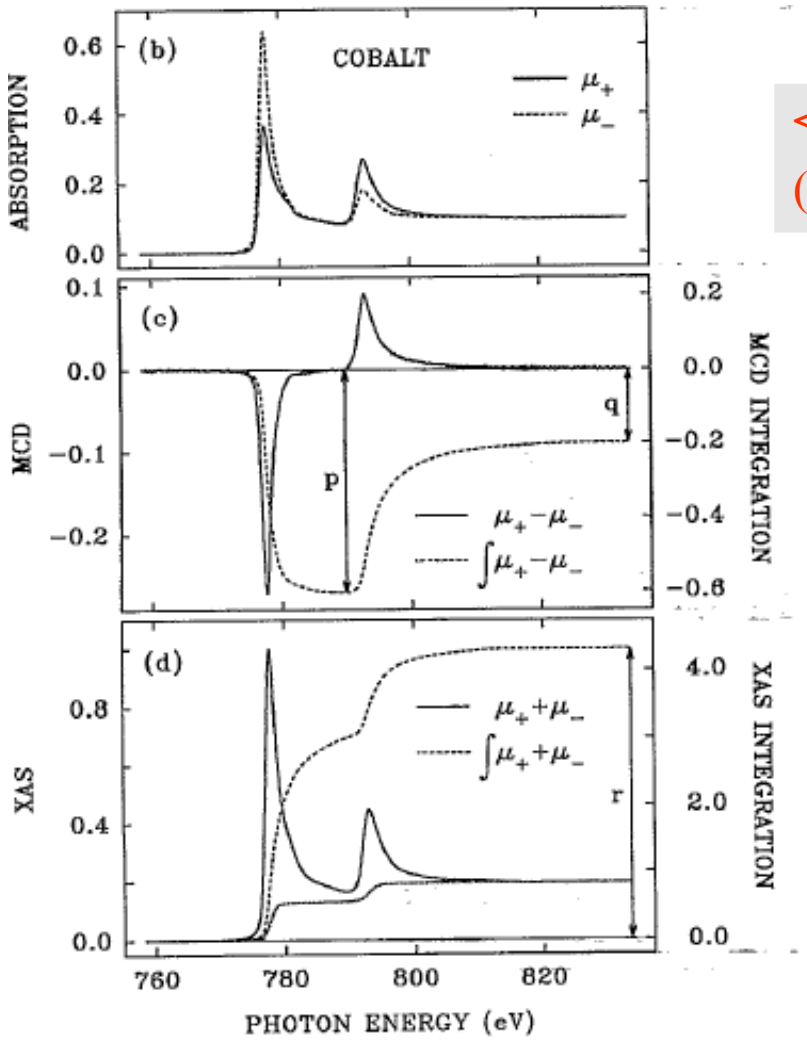

$$\langle S_Z \rangle + (7/2)\langle T_Z \rangle = (3/2)(10-n)[(\Delta L3 - 2\Delta L2)/\int_{L3+L2} d\omega\,(\mu_+ + \mu_- + \mu_0)]$$

$$= (3/2)(10-n)(p - 2\,(q-p))/(3/2)r =$$

$$= (3p - 2q)(10-n)/r$$

C.T.Chen *et al.*, PRL 75, 152 (1995)

XMCD sum rules : some precautions

- Background subtraction to separate 2p → 3d from other transitions

- Number of holes *n* not accurately known

- T_z can be important in low-dimensional systems

- For application of spin sum rule, L_3 and L_2 edges have to be sufficiently separated.

XMCD sum rules : application to Pd/Fe multilayers

- **Pd(X) / Fe(8 ML) with X=2,4,8,14 ML on MgO(001)**

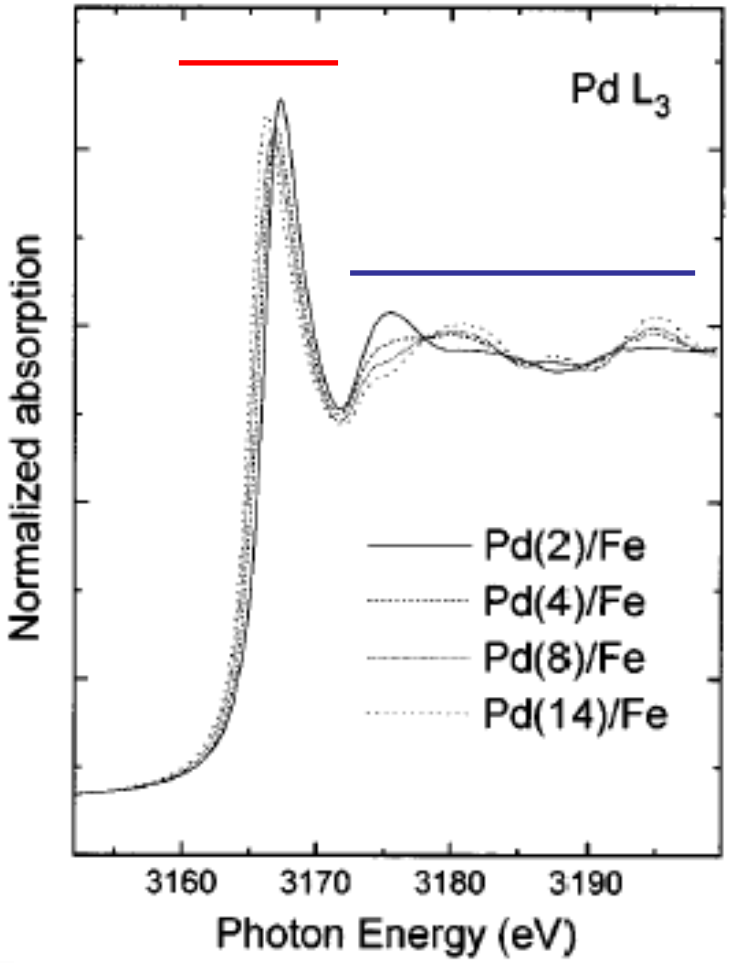

Peak position, intensity: electronic properties

Oscillations after peak : crystallographic structure

J. Vogel et al., Phys.Rev.B 55, 3663 (1997)

XMCD sum rules : application to Pd/Fe multilayers

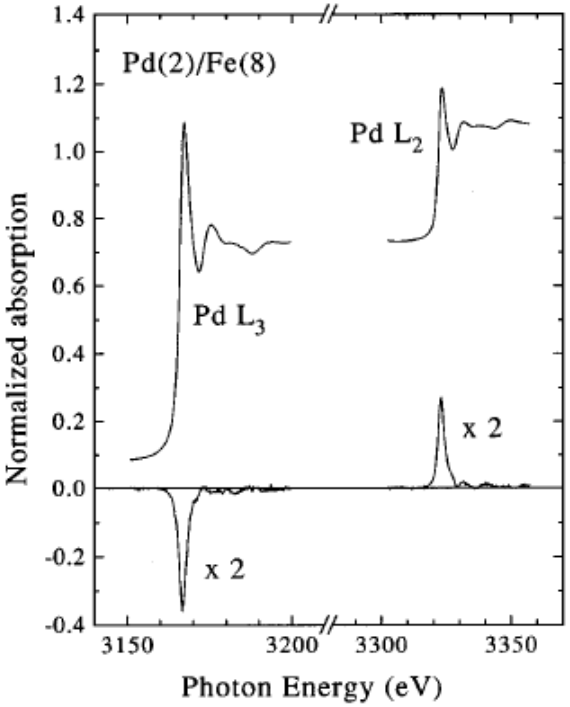

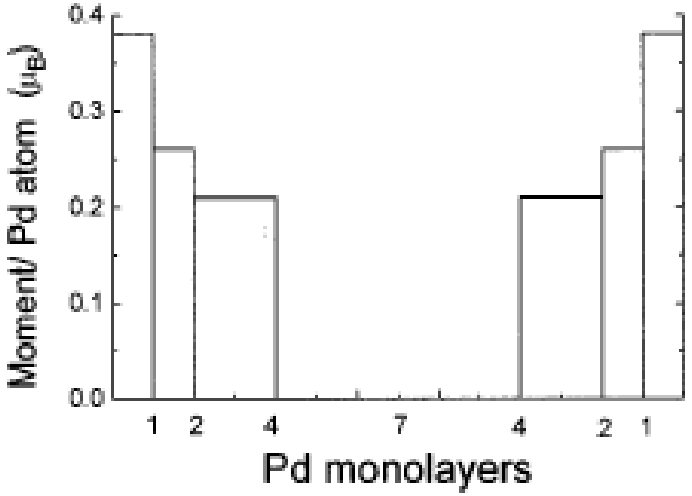

TABLE I. Values for orbital, spin, and total moments per Pd atom for the different multilayers. The values are obtained using sum rules on our circular dichroism data.

	$\langle L_z \rangle$ (μ_B)	$\langle S_z \rangle$ (μ_B)	Total moment (μ_B)	$\langle L_z \rangle / \langle S_z \rangle$
Pd(2 AL)/Fe(8 AL)	0.04±0.01	0.17±0.04	0.38±0.08	0.25±0.02
Pd(4 AL)/Fe(8 AL)	0.02	0.15±0.03	0.32±0.06	0.13
Pd(8 AL)/Fe(8 AL)	0.02	0.12±0.03	0.27±0.06	0.16
Pd(14 AL)/Fe(10 AL)	0.01	0.07±0.02	0.15±0.04	0.09

J. Vogel et al., Phys.Rev.B 55, 3663 (1997)

XMCD sum rules : Orbital magnetic moments and anisotropy

Perpendicular Magnetic Anisotropy ↔ magnetocrystalline anisotropy (MCA) (symmetry breaking and strain at the interface)

$E_A \propto - \xi (m_{orb}^{\perp} - m_{orb}^{\parallel})$ (Bruno, Phys.Rev.B 39, 865 (1989))

first experimental demonstration of orbital moment anisotropy

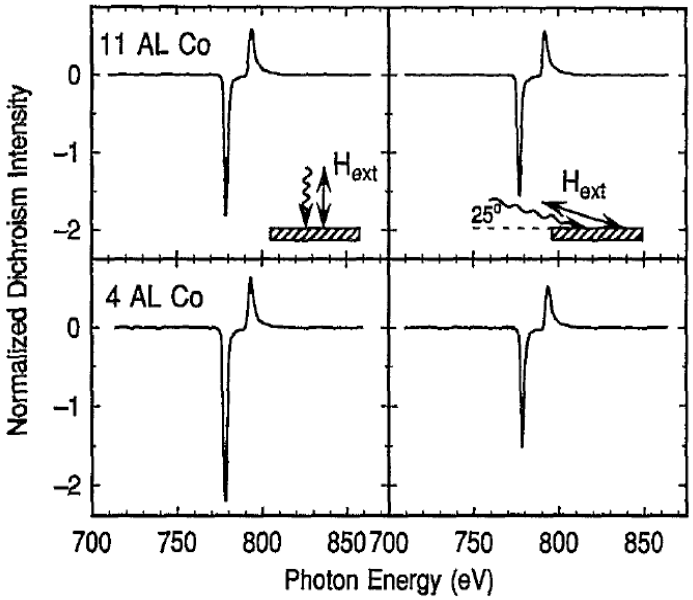

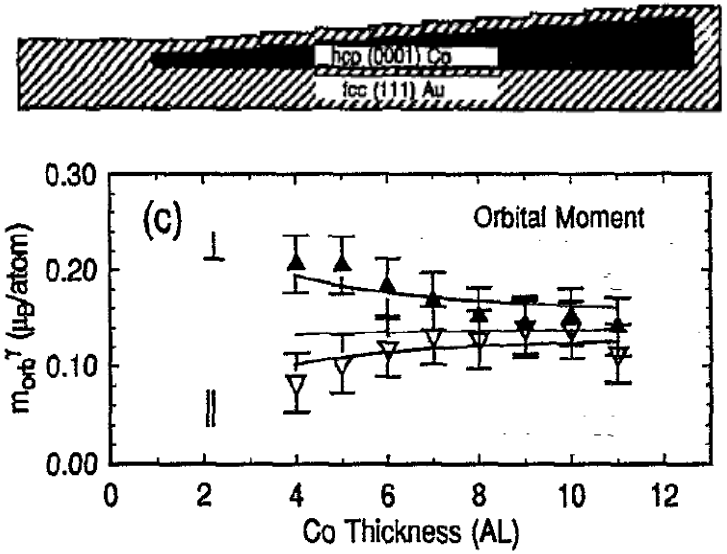

D.Weller et al., Phys. Rev. Lett. 75 (1995)

XMCD sum rules : Orbital magnetic moments and anisotropy

Single Co adatoms and particles MBE deposited on Pt(111) surfaces

P. Gambardella *et al*., Science 300, 1130 (2003)

STM image of isolated Co adatoms (8.5 nm x 8.5 nm)

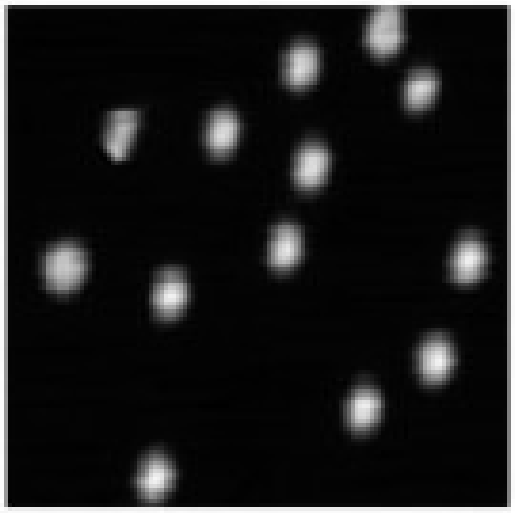

Large difference of in-plane and out-of-plane saturation field : very large Magnetic Anisotropy Energy

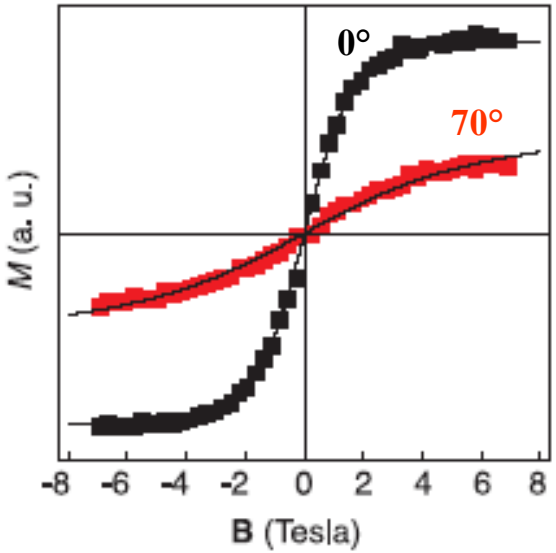

XMCD sum rules : Orbital magnetic moments and anisotropy

Single Co adatoms and particles MBE deposited on Pt(111) surfaces

P. Gambardella *et al*., Science 300, 1130 (2003)

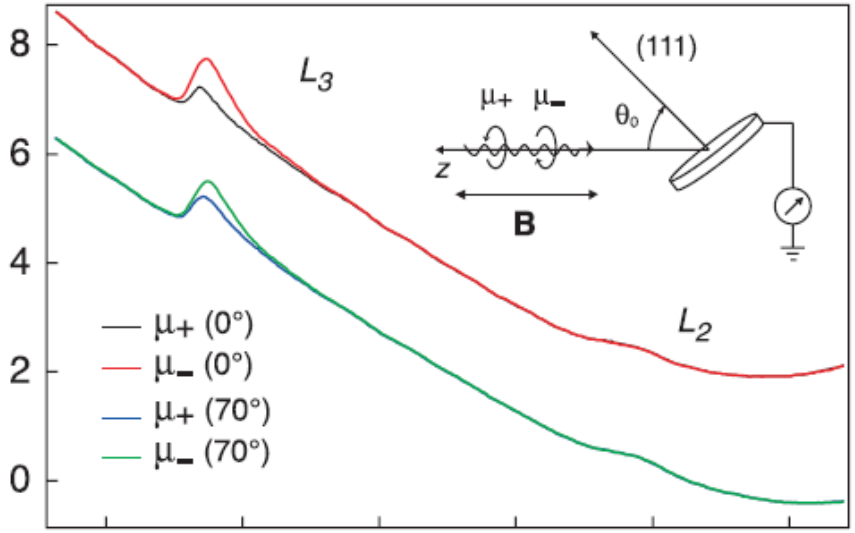

Co $L_{2,3}$ X-ray absorption spectra for 0° and 70°

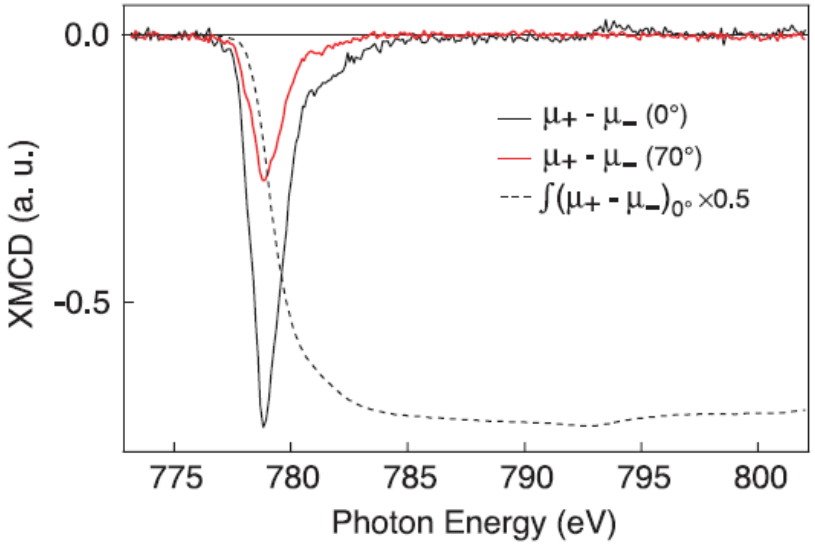

vanishing L_2 XMCD: very large orbital magnetism

XMCD sum rules : Orbital magnetic moments and anisotropy

Single Co adatoms and particles MBE deposited on Pt(111) surfaces

P. Gambardella *et al*., Science 300, 1130 (2003)

Sum rules : $\langle L \rangle = 1.1 \pm 0.1\ \mu_B$ for isolated Co adatoms ($L = 0.15\ \mu_B$ Co-hcp)
($L = 0.29\ \mu_B$ 1ML Co/Pt)

Reduced coordination of isolated atoms on top of a flat surface → d-electron localisation, increase of atomic character

From element-selective XMCD magnetization curves (up to 7 Tesla):
very large magnetic anisotropy energy (MAE)

$K = 9.3 \pm 1.6$ meV/atom

($K = 1.8$ meV/Co atom in $SmCo_5$)
($K = 0.3$ meV/atom in Pt/Co multilayers)

XMCD sum rules : Orbital magnetic moments and anisotropy

P. Gambardella *et al.*, Science 300, 1130 (2003)

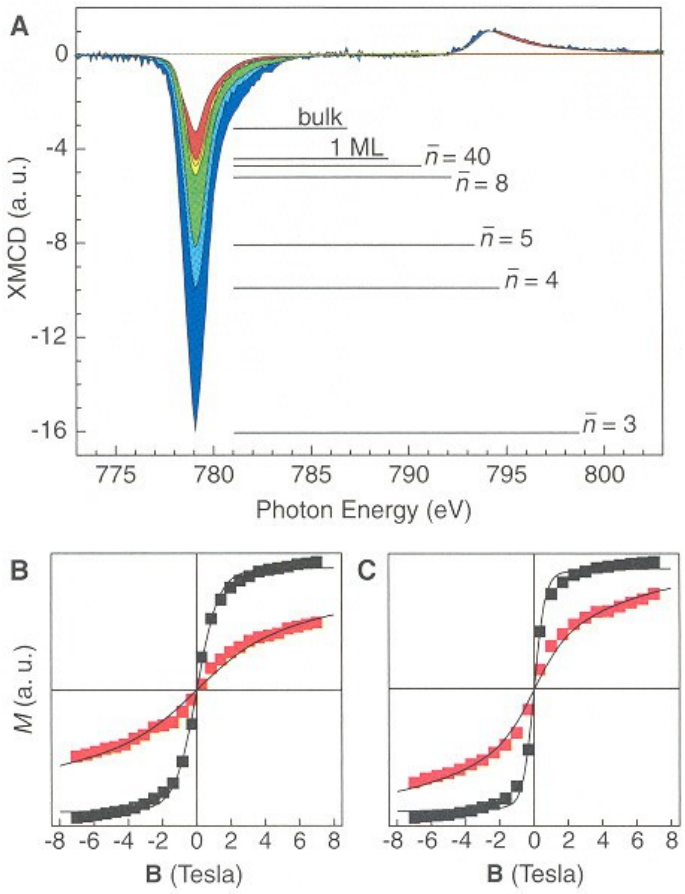

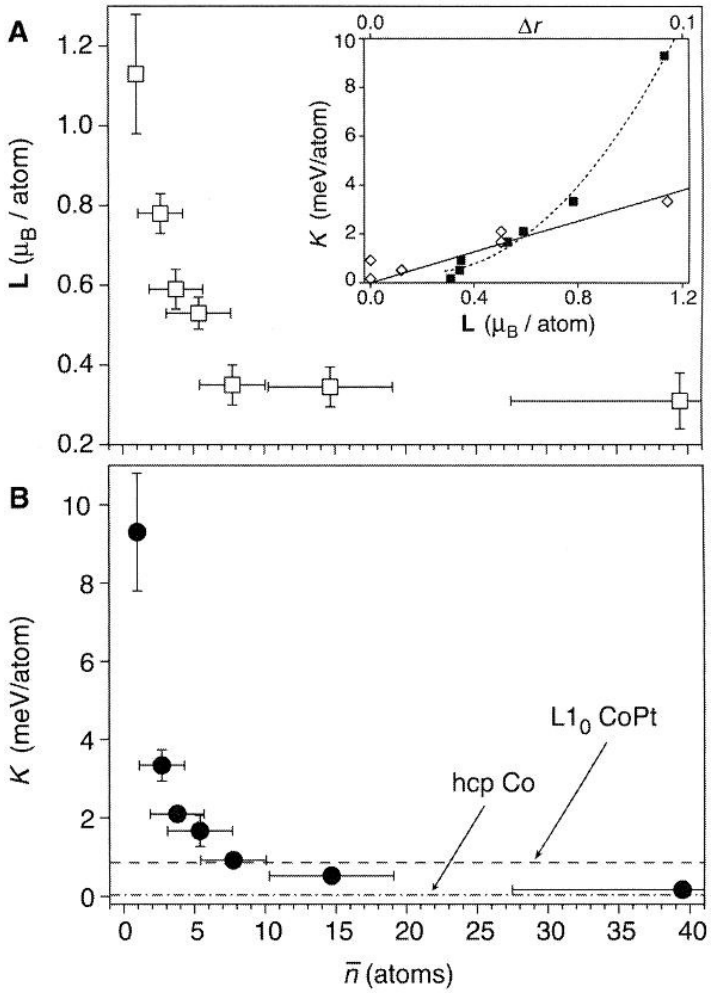

Increase of particle size : progressive quenching of orbital moment and consequent decrease of MAE

PHYSICAL REVIEW B **91**, 174426 (2015)

Twisted phase of the orbital-dominant ferromagnet SmN in a GdN/SmN heterostructure

J. F. McNulty,[1,*] E.-M. Anton,[1] B. J. Ruck,[1] F. Natali,[1] H. Warring,[1] F. Wilhelm,[2] A. Rogalev,[2] M. Medeiros Soares,[2] N. B. Brookes,[2] and H. J. Trodahl[1]

[1]*The MacDiarmid Institute for Advanced Materials and Nanotechnology, School of Chemical and Physical Sciences, Victoria University of Wellington, P.O. Box 600, Wellington, New Zealand*

[2]*ESRF-The European Synchrotron, CS40220, F-38043 Grenoble Cedex 9, France*

Sm $M_{4,5}$-edges, $\mu_0 H = 4T$

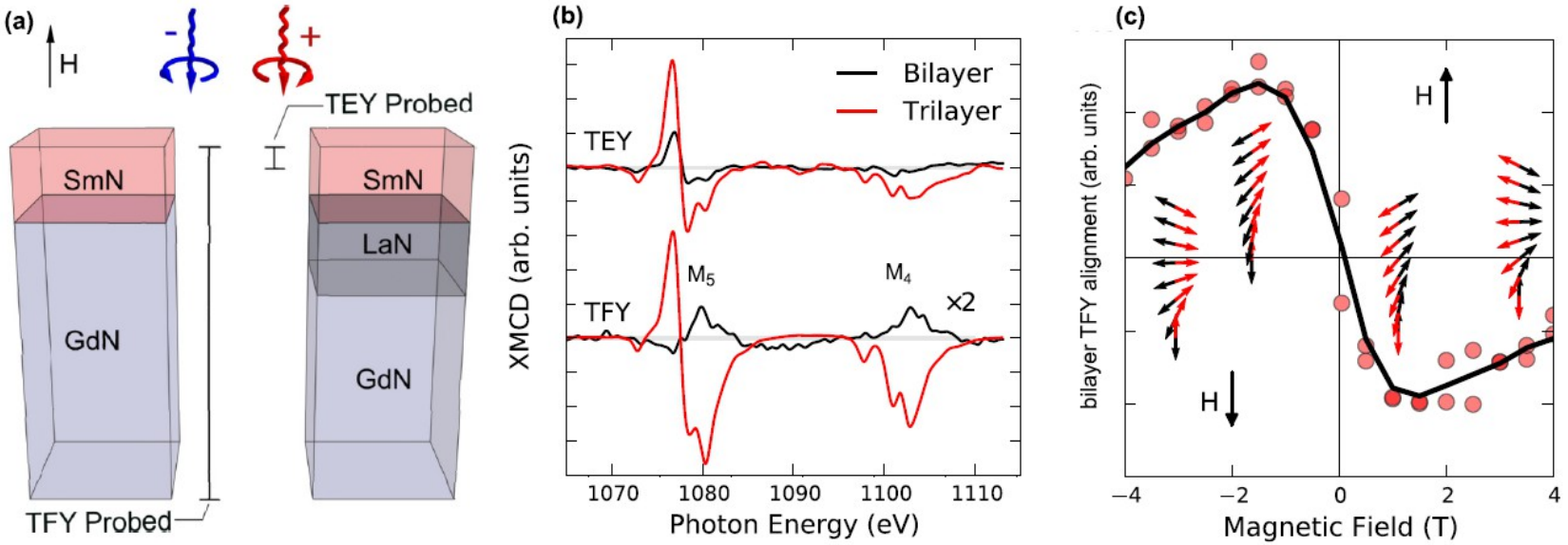

5.5 nm of SmN
Probing depth Total Electron Yield ~ 2-3 nm
Probing depth Total Fluorescence Yield ~ 100-200 nm